

Estimation of tropospheric ozone production using concentrations of hydrocarbons and NO_x , and a comprehensive hydrocarbon reactivity parameter

L. Allison Barrett^a, Nigel J. Bunce^{b,*}, Terry J. Gillespie^a

^a Department of Land Resource Science, University of Guelph, Guelph, Ontario, Canada N1G 2W1

^b Department of Chemistry and Biochemistry, University of Guelph, Guelph, Ontario, Canada N1G 2W1

Received 22 May 1997; accepted 22 September 1997

Abstract

We have developed a photochemical model for calculating the ozone concentration in a near-stationary air mass in the lower troposphere using data on chemical composition from August 1993, in the Village of Hastings, Ontario. The calculated concentration of ozone as a function of time was in good agreement with experiment for these data sets, except during incursions of air masses of different origin. Consideration of the mechanism of ozone formation allowed the ozone-forming potential of all hydrocarbons to be considered as a group, rather than using empirical values of ozone molecules formed per substrate molecule destroyed for each individual hydrocarbon. Use of the model predictively indicated that changes in NO_x concentration and light intensity had much greater impact upon the calculated ozone concentration than changes in relative humidity and hydrocarbon concentrations. The dependence of ozone concentration upon temperature was almost entirely due to thermal decomposition of peroxyacetyl nitrate (PAN), which adds to the reservoir of NO_2 on hot days. © 1998 Elsevier Science S.A.

Keywords: Photochemical modelling; Hydroxyl radicals; Ozone; Air pollution

1. Introduction

The formation of ground level oxidants remains a vexing problem in many jurisdictions. 'Ozone episodes', in which local concentrations of ground level ozone exceed regulatory limits, are common when polluted urban air matures photochemically under warm, sunny conditions, with maximal concentrations of ozone usually encountered in rural areas down-wind of the urban source. Adverse respiratory effects in humans and reduced agricultural yields are due to toxic components such as ozone and organic nitrates.

Three kinds of studies aid our understanding of the maturation of urban air pollution: actual monitoring of the concentrations of reactive species, e.g., Ref. [1]; smog chamber experiments in which synthetic polluted air is matured in the laboratory and the concentrations of reactants and products are monitored with time; and modelling studies, in which the maturation process is calculated, e.g., Ref. [2]. In a smog chamber experiment, the total mass of chemical substances is constant, and the measured concentrations of the reactants

and chemical products are followed with time. These may be compared with a theoretical model in which the input parameters are light intensity and the rate constants for all significant chemical processes occurring in the chamber. A mass balance cannot be achieved outdoors because reactants and products continually enter and leave the region advectively.

Models differ in the extent to which they rely upon empirical constants, as opposed to derivation from first principles, but all require more or less detailed knowledge of solar intensity and the rate constants for relevant chemical reactions as functions of temperature. Ultimately, they depend on the availability of reliable data sets obtained in the field for input and validation. An important recent advance is the development of comprehensive sets of chemical and climatic data in which hourly, or more frequent, measurements have been made of temperature (T), relative humidity, windspeed and direction, solar intensity, and the concentrations of important species such as nitrogen oxides and oxidizable substrates such as hydrocarbons, CO, and SO_2 .

In this work, we used experimental data from SONTOS (Southern Ontario Oxidants Study) [1], which was carried out at a rural site northeast of Toronto, Ontario, Canada in the summer of 1993. Our objective was to develop a model

* Corresponding author. Tel.: +1-519-824-4120 Ext. 3962; fax: +1-519-766-1499; e-mail: bunce@chembio.uoguelph.ca

that would treat the concentration of ozone as the only dependent variable; the experimental concentrations of all other substances with time were used as the input parameters. In this approach, we attempted to include only the major chemical processes and to avoid, as far as possible, having to estimate the concentrations of reactive intermediates. Because the present version of the model does not consider advection, it was validated against field data for days when the climatic conditions involved high pressure and light winds.

2. Tropospheric ozone

Ozone is a natural atmospheric constituent, occurring in the unpolluted troposphere at concentrations in the range 10–50 ppbv. Downward transport from the stratosphere and in situ photochemical formation in the troposphere are comparably important sources of tropospheric ozone [3]. The photochemical formation of tropospheric ozone in the unpolluted troposphere involves the null cycle of Scheme 1, from which the concentration of O₃ can be determined by the concentrations of the reaction partners and the intensity of sunlight [4].

Scheme 1:



The steady-state concentration of ozone predicted from Scheme 1 is significantly altered by the concurrent oxidation of oxidizable substrates such as hydrocarbons, CO, and SO₂, under conditions that the troposphere contains significant concentrations of NO_x. This is illustrated for oxidation of carbon monoxide, whose mechanism is a radical chain reaction that begins with attack on the substrate by hydroxyl radicals (Scheme 2, in which reaction in Eq. (7) is a summary equation for reactions in Eqs. (1) and (2)).

Scheme 2:



Overall reaction: $\text{CO} + 2\text{O}_2 + h\nu \rightarrow \text{CO}_2 + \text{O}_3$.

In practice, the accumulation of ozone is less than predicted from Scheme 2 [5–8], because HO₂ is also reduced to OH by reaction with O₃; reaction in Eq. (8). The relative rates of reactions in Eqs. (6) and (8) therefore determine to what extent substrate oxidation is an ozone-forming or an ozone-depleting process.



Overall reaction in Eq. (4) + Eq. (5) + Eq. (8): $\text{CO} + \text{O}_3 \rightarrow \text{CO}_2 + \text{O}_2$

3. Model development

The goal of this research was to develop a simple model for the production of ozone when parameters such as temperature and the concentrations of the various reactants were known from experimental measurements. The principle of a non-advective kinetic model is to catalog the rates of all important chemical and photochemical reactions over successive small time intervals. The incremental disappearance of reactant species and appearance of product species for each reaction is calculated, allowing the chemical maturation of the air mass to be predicted. This process requires the concentrations of all reactant species to be known, along with the chemical or photochemical rate constant for every process. Excellent compilations of rate constants are now available [9,10], and data sets comprising the concentrations of species such as CO, NO, NO₂, O₃, and many hydrocarbons, measured at frequent time intervals, have recently become available. Such data sets, including the SONTOS data used in the present work, allow comparison between calculation and experiment.

Many practical difficulties remain, however. 'First principles' approaches not only require the inclusion of very extensive sets of chemical and photochemical reactions, but also require experimental or estimated values of the concentrations of reactive radical species such as H, OH, HO₂, and their organic homologs R, RO, and RO₂. These are at or below current analytical detection limits, and were not available in the SONTOS data. In addition, the experimental concentrations of the various reaction partners are usually measured using instruments situated near ground level; these do not accurately reflect the concentrations in the tropospheric boundary layer (height < ca. 1 km) because the ground is a strong sink for reactive gases such as O₃ and NO₂ [11,12]. This has been strikingly illustrated for data obtained in central Toronto, Ontario where completely different concentrations of NO_x and O₃ have been measured at the top of the 'CN Tower' at 444 m elevation and at a nearby monitoring station at street level (Annette Deane, Personal Communication, MOEE Air Resources Branch, as cited in N.J. Bunce, H.G. Dryfhout, *Can. J. Chem.*, 70 (1992), 1966–1970). Ground level sinks produce concentration gradients in the lowest 100 m, and therefore, models that employ data collected near ground level can only reflect trends rather than absolute concentrations in the chemistry of the tropospheric boundary layer. In this work, we sought to develop a model that would avoid the need for explicit values of unobtainable concentrations but still allow the user to make predictions about the behaviour of a given air mass rapidly and conveniently.

We consider an oxidizable substrate S that yields Φ molecules of ozone per molecule of S oxidized. Bimolecular attack on S by OH is usually the predominant reaction channel

(rate constant k_5); hence, the rate of forming ozone is given by Eq. (9). Eq. (10) gives the yield of ozone for a mixture of many oxidizable substrates and a time interval Δt .

$$+d[\text{O}_3]/dt = \Phi k_5 [\text{S}] [\text{OH}] \quad (9)$$

$$+\Delta[\text{O}_3] = \Sigma(\Phi k_5 [\text{S}]) [\text{OH}] \Delta t \quad (10)$$

The concentration of OH is rarely available experimentally, due to difficulties in measurement [13,14], and must be estimated. This was done by assuming an instantaneous steady state of OH (Eq. (11)) and calculating the rate of formation of OH; this approach is reasonable in view of the short half-life of OH in the troposphere [15]. 'Sink' in Eq. (11) represents any substance which removes OH from the atmosphere. 'Sink' is not equivalent to the oxidizable substrates of Eq. (9) however, because the chain reactions involving the oxidizable substrates regenerate hydroxyl radicals (Scheme 2).

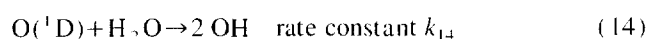
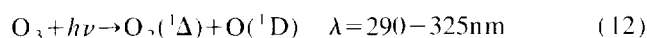
OH formation rate = OH destruction rate

$$= \Sigma k [\text{sink}] [\text{OH}] \quad (11)$$

$$\therefore [\text{OH}] = (\text{OH formation rate}) / \Sigma(k [\text{sink}])$$

The rate of forming OH can be calculated from the reaction mechanism for forming OH (Scheme 3).

Scheme 3:



The rate of ozone photolysis = $J(\text{O}_3) \times [\text{O}_3]$ can be calculated from the observed concentration of ozone and the photochemical rate constant $J(\text{O}_3)$. Calculation of $J(\text{O}_3)$ requires knowledge of the solar intensity (J) in the relevant spectral range, along with the absorption cross-section of ozone (σ) and the quantum yield (ϕ) for cleavage of ozone to excited (^1D) oxygen atoms. Tabulations of these parameters, all of which are wavelength dependent, are available from the literature at specified zenith angles, Z [16]. $J(\text{O}_3)$ can be calculated at a tabulated value of Z , using Eq. (15) [17]. Because Z changes with the geographical latitude, date, and time of day, values of $J(\text{O}_3)$ intermediate between the tabulated values of Z are estimated by fitting to a cosine function (Eq. (16), in which m has the empirical value 2.4 except when Z is near 90° [17]. An experimental correction is needed for cloud cover (β , a factor between 0 and 1), reflecting that the intensity of UV scales approximately with total light intensity [18]

$$J(\text{O}_3) = \beta \Sigma(I_{\lambda,Z} \sigma_\lambda \phi_\lambda) \quad (15)$$

$$J(\text{O}_3)_Z = J(\text{O}_3)_{Z=0} (\cos Z)^m \quad (16)$$

Using Scheme 3, the rate of forming [OH] is given by Eq. (17), and so substitution into Eq. (11) gives Eq. (18).

$$+d[\text{OH}]/dt = 2\beta J(\text{O}_3) [\text{O}_3] \frac{k_{14} [\text{H}_2\text{O}]}{k_{13} + k_{14} [\text{H}_2\text{O}]} \quad (17)$$

$$[\text{OH}] =$$

$$2\beta J(\text{O}_3) [\text{O}_3] \frac{k_{14} [\text{H}_2\text{O}]}{k_{13} + k_{14} [\text{H}_2\text{O}]} \frac{1}{\Sigma k [\text{sink}]} \quad (18)$$

Eq. (18) predicts the concentration of OH to be directly related to the rate of photolysis of ozone, provided that $[\text{H}_2\text{O}]$ and $\Sigma k \times [\text{sink}]$ vary little with time. Bunce et al. [17] showed that these conditions held for the experimental data set published by Platt et al. [19] for a remote location. However, the results of Dorn et al. [20] show that a simple linear relationship between $R(\text{O}_3)$ and $[\text{OH}]$ is invalid in a polluted atmosphere, because high concentrations of NO_2 effectively titrate OH out of the atmosphere, the reaction in Eq. (19). Under these (urban) conditions, NO_2 appears to be the strongest 'sink', and the reaction of OH with NO_2 must be considered explicitly, Eq. (20). At sufficiently high $[\text{NO}_2]$, the term $k_{19} [\text{NO}_2]$ predominates over the remaining 'sink' reactions. In this work we used $\Sigma k [\text{sink}] = 0.3 \text{ s}^{-1}$ as an empirical value that we derived from the Platt et al. and the Dorn et al. data sets.



$$[\text{OH}] = 2\beta J(\text{O}_3) [\text{O}_3] \frac{k_{14} [\text{H}_2\text{O}]}{k_{13} + k_{14} [\text{H}_2\text{O}]} \times \frac{1}{\Sigma k [\text{sink}] + k_{19} [\text{NO}_2]} \quad (20)$$

4. Change in ozone concentration

The contributing reactions to the change in ozone concentration during a time increment Δt are (a) loss of ozone through photolysis, (b) loss of ozone by reaction with NO: the reaction in Eq. (3), (c) formation of ozone following photolysis of NO_2 , and (d) formation of ozone by reaction with oxidizable substrates (Scheme 2).

Contribution (a): This is calculated from Scheme 3, noting that the reaction in Eq. (13) is followed immediately by the re-formation of ozone by reaction of $\text{O}(^3\text{P})$ with O_2 .

$$\Delta[\text{O}_3]_a = - \left(\beta J(\text{O}_3) [\text{O}_3] \frac{k_{14} [\text{H}_2\text{O}]}{k_{13} + k_{14} [\text{H}_2\text{O}]} \right) \Delta t \quad (21)$$

Contribution (b):

$$\Delta[\text{O}_3]_b = -k_3 [\text{NO}] [\text{O}_3] \Delta t \quad (22)$$

Contribution (c): The rate of photolysis of NO_2 , which is calculated in the same manner as the rate of photolysis of ozone.

$$\Delta[\text{O}_3]_c = J(\text{NO}_2) [\text{NO}_2] \Delta t \quad (23)$$

Contribution (d): Substitute Eq. (20) into Eq. (10).

$$\Delta[\text{O}_3]_d = (\beta J(\text{O}_3)[\text{O}_3] \frac{k_{14}[\text{H}_2\text{O}]}{k_{13} + k_{14}[\text{H}_2\text{O}]} \times \frac{\{2\sum\Phi k_s[S]\}}{\sum k[\text{sink}] + k_{19}[\text{NO}_2]} \Delta t \quad (24)$$

We note that contribution (d) does not duplicate contribution (c) because of the way the model is run. At each time increment, the calculation uses the measured concentration of all substances except ozone. The disturbance of the NO:NO₂ ratio that accompanies substrate oxidation in the *i*th time increment would not yield ozone until the extra NO₂ was photolyzed in the (*i* + 1)th time increment, at which point the concentration was set back to its experimental value. The incorporation of contribution (d) allows the inclusion of this source of ozone in the model.

In Eq. (24) the values of Φ vary with the substrate and with the maturity of the air mass and the NO_x: substrate ratio due to the different kinetic reactivities of the substrates [5]. It is cumbersome to apply Eq. (24) when each oxidizable substrate has its own Φ value, and even more difficult to decide which values of Φ are most relevant to a given environmental case.

Plots of the various Φ values in the literature against each other gave approximately linear correlations having r^2 values > 0.7 (data not shown). This correlation exists because the oxidations of all substrates are similar mechanistically: in step 1, OH either adds to the substrate or abstracts hydrogen from it; in step 2, O₂ removes a hydrogen atom from a radical intermediate, to form HO₂. Whether ozone is formed or destroyed depends on whether the HO₂ radical reacts with NO (reactions in Eqs. (6) and (7)) or ozone (reaction in Eq. (8)), and not on the properties of individual oxidizable substrates; the yield of ozone depends on $f = (k_6[\text{NO}]) / \{k_6[\text{NO}] + k_8[\text{O}_3]\}$, the fraction of HO₂ radicals that react with NO. Defining $\Phi' = 2f - 1$, exclusive reaction of HO₂ with NO gives $\Phi' = +1$; exclusive reaction with O₃, $\Phi' = -1$; equal reactivities with NO and O₃, $\Phi' = 0$. Eq. (24) is thereby modified to Eq. (25), in which Φ' is a property of the air mass rather than of an individual oxidizable substrate.

$$\Delta[\text{O}_3]_c = (\beta J(\text{O}_3)[\text{O}_3] \frac{k_{14}[\text{H}_2\text{O}]}{k_{13} + k_{14}[\text{H}_2\text{O}]} \times \frac{\{2\Phi'\sum k_s[S]\}}{\sum k[\text{sink}] + k_{19}[\text{NO}_2]} \Delta t \quad (25)$$

This approach avoids two problems: the need to locate a Φ value for each oxidizable substrate, and the variation of Φ with the maturity of the air mass [5]. The latter issue is accounted for by the use of the individual rate constants k_s in Eq. (25).

5. Methods

Comprehensive sets of atmospheric and analytical chemical data were available for the Village of Hastings, Hastings

County, Ontario [1] for the summer of 1993 (Fig. 1 shows a sketch of part of southern Ontario, Canada). The model was tested using data from 3 days in August 1993, by comparing the measured values for the ozone concentration with those calculated by summing the various contributions to the change in the ozone concentration at 5 min intervals. Measured concentrations of NO_x, CO and SO₂, relative humidity, and light intensity, were available at 5 min intervals, but those of the following hydrocarbons were available at approximately 1 h intervals during the day and were assumed to be constant between measurements: ethane, propane, *n*-butane, *i*-butane, *n*-pentane, *i*-pentane, *n*-hexane, 2-methylpentane, 3-methylpentane, *n*-octane, ethene, propene, 1-butene, *i*-butene, 1-pentene, isoprene, benzene, toluene, *o*-xylene, (*m* + *p*)-xylene. For ozone, only the initial measured concentration was input for each day.

6. Results and discussion

Fig. 2 shows the comparison between experimental and modelled concentration of ozone for August 25 (panel a), 26 (panel b) and 27 (panel c). On each day, the starting ozone concentration was set equal to the experimental value at the start of the day, after which the experimental and calculated values were allowed to diverge. Of the 3 days modelled, August 25 was ideally suited to the non-advective approach, with wind speeds at 10 m elevation consistently < 12 km h⁻¹ (averaging < 6 km h⁻¹) and without a consistent direction. The calculated and measured ozone concentrations were consistently within 7 ppbv. The results were indistinguishable ($\pm 2-3$ ppbv) whether we used Eq. (25) or the individual Φ values of Chameides et al. [7], Eq. (24).

Certain events on August 26 and 27 could not be modelled satisfactorily with the non-advective approach, and Fig. 2B,C show substantial differences between observed and estimated ozone concentrations at certain periods on those days. These deviations are ascribed to incursions of different air masses,

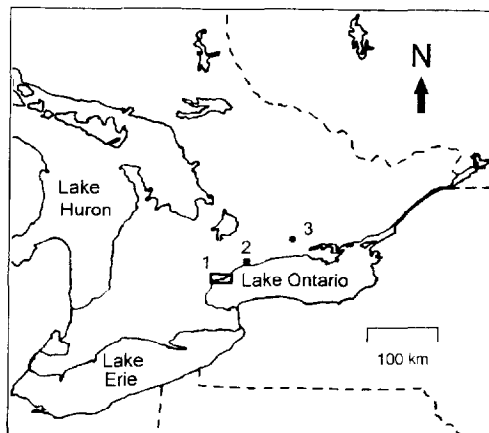


Fig. 1. Sketch of part of southern Ontario, Canada, showing the locations of Hastings (3), Oshawa (2), and Toronto (1).

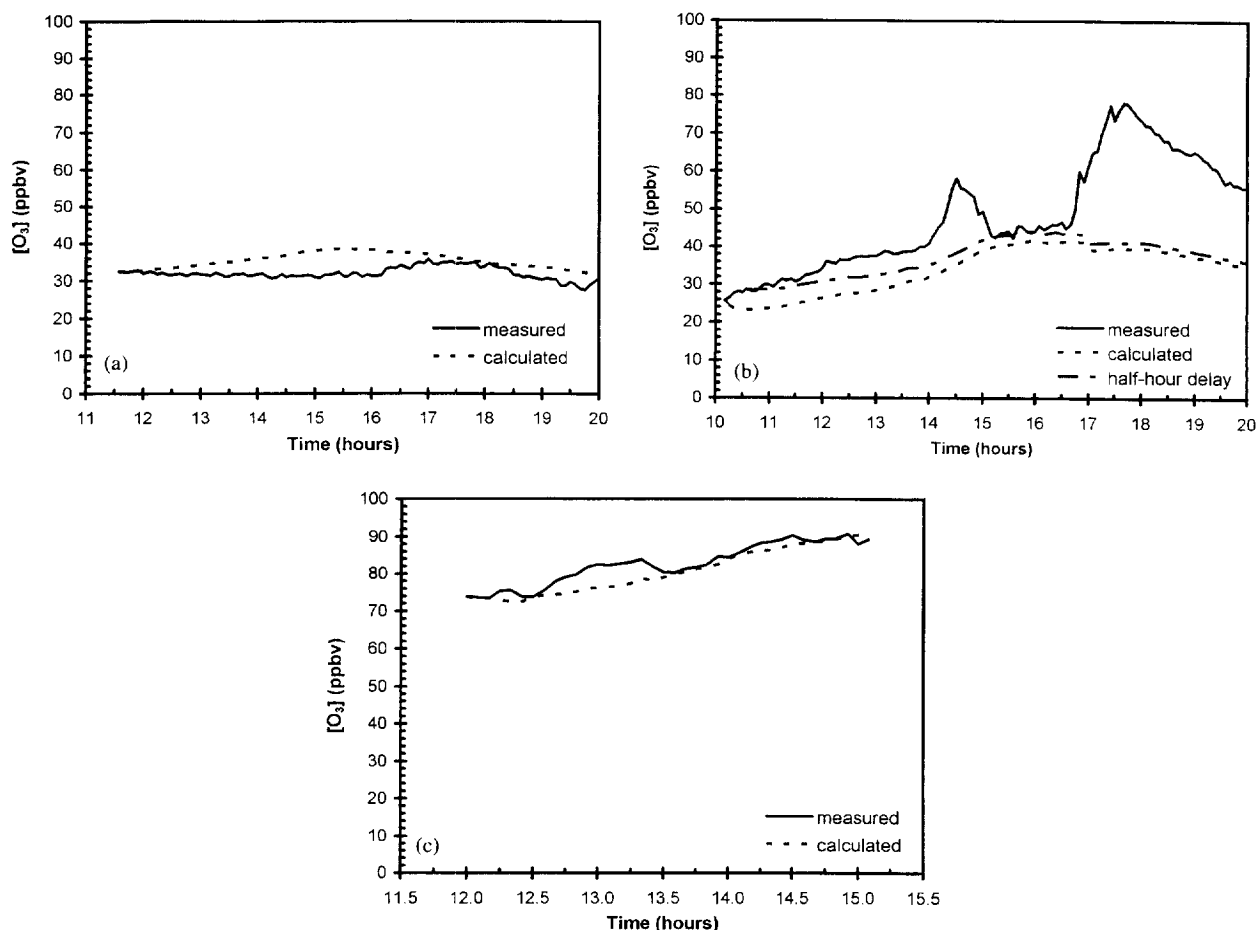


Fig. 2. Measured and calculated ozone concentrations at Hastings, Ontario for (A) August 25, (B) August 26, and (C) August 27, 1993.

as reflected in shifts in both wind speed and direction during these episodes.

On August 26, a lake breeze front passed through the Hastings site at approximately 16.75 EDT [21]. This incursion of air was characterized by an increase in wind speed from 2 to 4 m s⁻¹, a temporary change in wind direction from westerly to southwesterly, and an increase in ozone concentration from 46 to nearly 80 ppbv (at 17.5 EDT), with simultaneous increases in the concentrations of NO_x, CO, PAN and SO₂. The smaller pulse in the ozone concentration earlier that day was also characterized by shifting wind direction (westerly to southwesterly) with simultaneous increases in PAN, NO_x and CO, but not SO₂.

The calculated values of ozone concentration early on August 26 showed a decrease that was not observed experimentally. This effect was traced to temporarily high concentrations of NO, which removes ozone through the reaction in Eq. (3). We suspect that the experimental increase in [O₃] was likely caused by temporarily greater production of OH by photolysis of HNO₂. This reaction is well known to be important early in the day due to overnight heterogeneous hydrolysis of NO₂ to HNO₂ [22]. The short and long dashed line in Fig. 2B shows the result of ignoring the first 30 min of the August 26 data, because we had no experimental infor-

mation on the atmospheric concentration of HNO₂ in the early morning. Apart from the lake breeze incursions, the subsequent estimation of ozone concentration for August 26 was within 4 ppbv of the measured values.

On August 27, a decrease in ozone concentration from 90 to 70 ppbv and a shift in the wind direction from west to northwest occurred between 15.0 and 15.3 EDT, just prior to a thunderstorm that swept through the area at 15.75 EDT. This episode was accompanied by decreased concentrations of NO_x, CO and SO₂, and would have the effect of mixing the air mass to elevations well above the previously established tropospheric boundary layer. Prior to this event the calculations for August 27 showed good agreement with measured ozone concentrations.

Calculations were then carried out in which one or more of the parameters such as relative humidity, [NO_x] or solar intensity was shifted from its experimental values, to predict how the concentration of ozone might have progressed in a similar air parcel on a hotter day, a more humid day, at a different time in the season, etc. In each case, the parameter to be varied was changed by a constant amount (e.g., increase [NO₂] by 0.2 ppbv or increase relative humidity by 10%) throughout the day of August 25 with all other variables kept at their measured values. Representative results are shown in

Fig. 3. Changes in the values of more than one parameter in a given run produced changes in the calculated ozone concentrations that were not always the sum of the changes predicted when a single parameter was changed.

6.1. NO_x

Even small variations in the concentration of either NO or NO_2 caused significant change in the calculated ozone con-

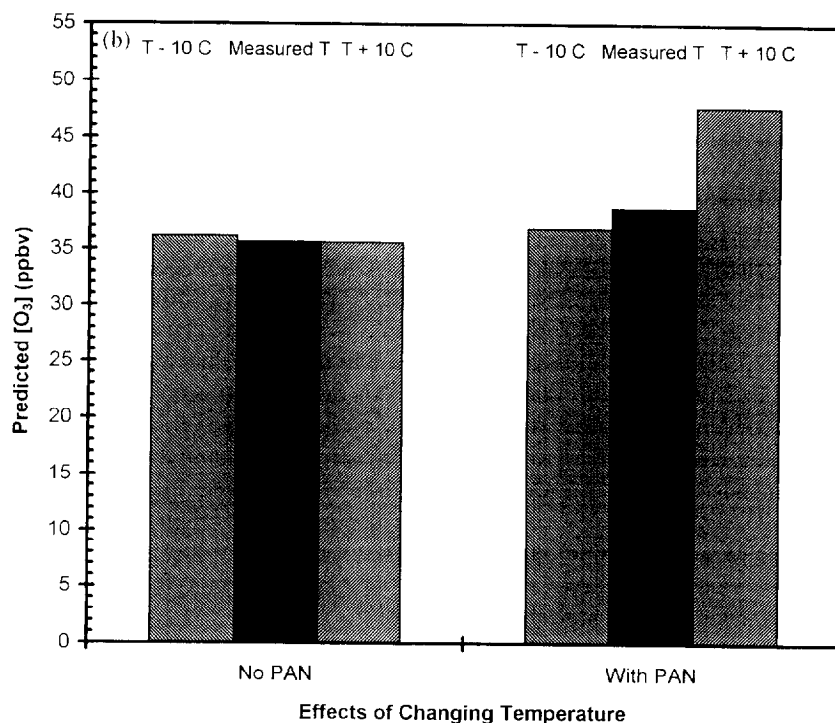
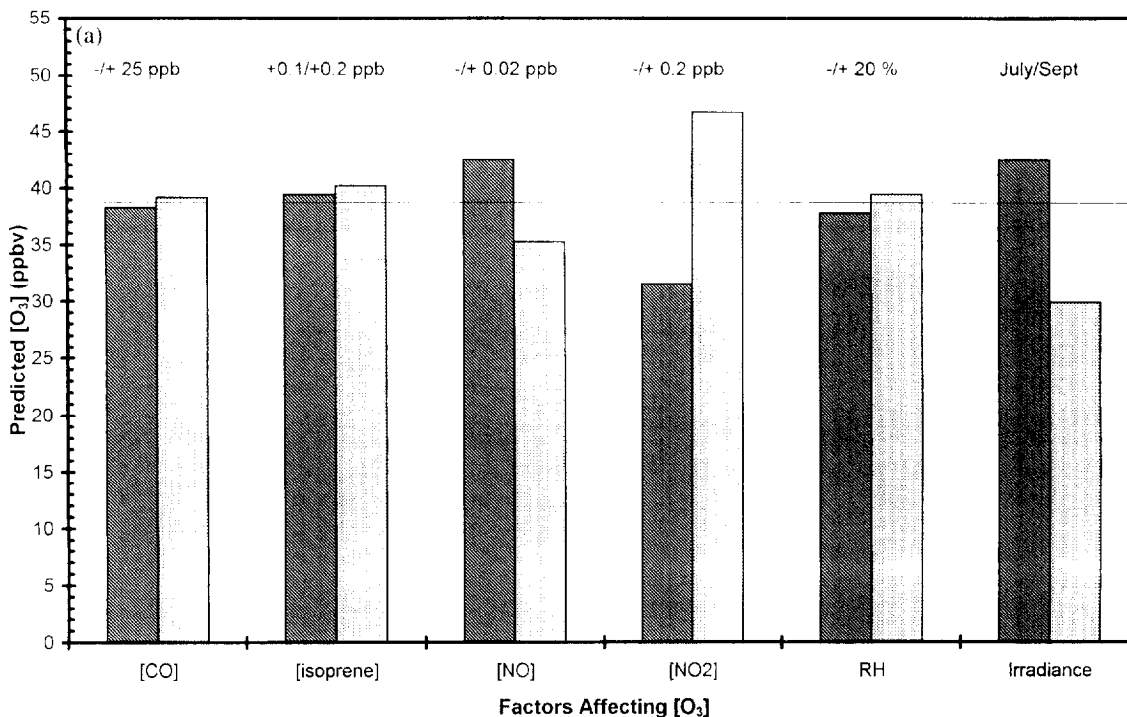


Fig. 3. Comparison of the calculated ozone concentration at Hastings, Ontario on August 25, 1993 under different conditions. The horizontal line — indicates the ozone concentration taken from Fig. 2A calculated at 16.083 h (4:05 pm) using measured values of [CO], [isoprene], [NO], [NO₂], relative humidity, temperature and solar irradiance. The bars show the calculated ozone concentration at the same time when the factors indicated were changed by the amounts indicated, with all other factors held at their measured values during these trials: relative humidity = 34.18%, [NO] = 0.217 ppbv, [isoprene] = 0.706 ppbv, [NO₂] = 0.252 ppbv, [CO] = 156 ppbv, temperature = 32.78°C. Panel B compares the result of changing the temperature with the dissociation of PAN excluded (left hand bars) or included (right hand bars) in the model.

centration. Increases in ozone were predicted if $[\text{NO}]$ decreased (reduction of the rate of reaction in Eq. (3)) or if $[\text{NO}_2]$ increased (increased rate of reactions in Eqs. (1) and (2)). The ground as a sink for NO_2 is expected to change the low-level (<10 m) concentration of both NO_x and ozone from their tropospheric boundary layer (<ca. 1 km) values to a significant, though unquantifiable, extent. A further small effect will be contributed by biological emissions of NO from soil (about $0.25 \text{ kg ha}^{-1} \text{ yr}^{-1}$; G. Thurtell, personal communication), in that NO emissions will rapidly be oxidized to NO_2 by reaction in Eq. (3), depleting ozone, and the NO_2 thus formed will be reabsorbed by soil.

Experimental evidence in support of a gradient in the concentration of ozone with altitude was provided on August 26, when the ground-based measurements were complemented by analyses from aircraft (Julie Narayan, York University, personal communication). These show ozone concentrations at 400 m altitude of 60–70 ppbv, at a time when the ground-based analyzers showed ~ 50 ppbv.

6.2. Hydrocarbons

Changes in $[\text{O}_3]$ were approximately linear with total [Hydrocarbon], but were small unless the hydrocarbon concentration changed by factors of at least 3, as might occur under highly polluted conditions. However, unsaturated hydrocarbons have much larger rate constants for reaction with OH than alkanes, and therefore have much larger photochemical ozone creation potentials. Selective removal of ethane, propane, butane, isobutane and pentane from the list of hydrocarbons had negligible effect (<1 ppbv) on the calculated ozone concentration on any of the 3 days modelled, whereas deletion of isoprene, benzene, toluene, and the xylenes reduced $[\text{O}_3]$ by several ppbv. For example, increases in [isoprene] as small as 0.1 ppbv had a greater effect than changing [CO] by 25 ppbv (Fig. 3), and this is consistent with the large value of Φ reported for isoprene [7].

6.3. Solar irradiance

Solar irradiance was changed by taking the reference date of August 25, and repeating the calculation for July 26 and September 25. Contributions (a), (c), and (d) to the ozone concentration all depend on light intensity. Contribution (d) favours ozone formation; contributions (a) and (c) are opposing terms which together show a small positive correlation with light intensity because the term $\{2\Phi' \cdot \Sigma k_s \cdot [S]\} / \{\Sigma k \cdot [\text{sink}] + k_{19} \cdot [\text{NO}_2]\}$ of Eq. (25) is somewhat greater than 1 (Eq. (21)).

6.4. Relative humidity

Water vapour is required for the formation of OH from ozone (reaction in Eq. (14)), but changes in relative humidity up to $\pm 30\%$ produced only small changes in the calcu-

lated ozone concentration. Again, this is because of the opposed directions and similar magnitudes of Eqs. (21) and (25), as just discussed.

6.5. Temperature

It is widely assumed that the parameters needed for photochemical ozone formation are [hydrocarbons], $[\text{NO}_x]$, sunlight, and temperature $> \text{ca. } 18^\circ\text{C}$. However, the model as described so far showed almost no dependence of $[\text{O}_3]$ on temperature (Fig. 3B). This is not easily predictable by examination of Eq. (21), (24), and (25) because of the interplay of the large number of rate constants. In Eq. (21), rate constant k_{13} decreases very slightly with temperature and k_{14} is constant between 200 and 350 K [9,10]. Therefore, the loss of ozone through photolysis is nearly independent of temperature. The loss of ozone by reaction with NO increases with temperature (rate constant k_3). In the ozone-forming process represented by Eq. (25), the factor $k_{14}[\text{H}_2\text{O}] / \{k_{13} + k_{14}[\text{H}_2\text{O}]\}$ is nearly independent of temperature (see above); k_{19} decreases slightly with temperature. Of the various contributors to Σk_s , the saturated hydrocarbons react faster at higher temperatures, and the unsaturated ones, which are more important ozone-formers, have negative temperature coefficients (typical of substrates that add OH rather than undergo hydrogen abstraction). The sum of these contributions leaves little dependence of ozone formation on temperature.

This picture is changed by considering the behaviour of PAN, which acts as a temporary sink for odd nitrogen. The rate constant for decomposition of PAN to NO_2 and $\text{CH}_3\text{CO}\text{OO}\cdot$ has a very steep temperature coefficient, implying that on hot days (especially when the temperature exceeds 30°C) a significant proportion of PAN is recycled to NO_2 , thereby boosting the production of ozone by the reaction in Eq. (7) [23]. We included this phenomenon in the model as follows. Consider the production of NO_2 caused by thermal decomposition of PAN at each time interval i , and add this increment of NO_2 to the measured concentration of NO_2 during time increment $(i+1)$, allowing extra ozone to be formed during time interval $(i+1)$. This effect is illustrated in Fig. 3B, and explains the increase of $[\text{O}_3]$ with temperature.

6.6. Wind speed

In a preliminary examination of meteorological factors, we observed empirically that the ozone yield was proportional to the average wind speed from the southwest (in the range $0\text{--}20 \text{ km h}^{-1}$; $r^2 > 0.97$). Higher wind speeds decrease the time taken for the air parcel to travel to Hastings from source regions such as Toronto, making it chemically 'younger' at the time of observation. We have already noted that on August 25 the wind speeds at 10 m elevation averaged $< 2 \text{ m s}^{-1}$, whereas on August 26 the wind speed from the southwest increased at the time of the two ozone events subsequent to

14 h and 17 h, in each case from $\sim 2 \text{ m s}^{-1}$ to $\sim 4 \text{ m s}^{-1}$. These events are consistent with the advection of younger air masses into the test zone. Examination of data from the Oshawa ozone-monitoring station of the Ontario Ministry of Environment, which is 86 km SW (upwind) of Hastings, showed an increase in ozone concentration at Oshawa 4 h ahead of the high ozone incursion at 16.75 h at Hastings. This explanation is only qualitative because the air parcel leaving Oshawa undoubtedly matured photochemically and also dispersed on its way to Hastings. Episodes such as this are impossible to model in the absence of complete chemical and climatic data at both the upwind site (Oshawa) and the primary test site (Hastings).

Acknowledgements

This work was sponsored by the Atmospheric Environment Service of Environment Canada, the Natural Sciences and Engineering Research Council of Canada and the Ontario Ministry of Agriculture Food and Rural Affairs (OMAFRA). We particularly thank Don Hastie and Ron Taylor of York University for their generosity in allowing us access to their comprehensive data sets obtained at Hastings, Ontario in the summer of 1993.

References

- [1] D.R. Hastie, P.B. Shepson, N. Reid, R.B. Roussel, O.B. McLo, *Atmos. Environ.* 30 (1996) 2157–2166.
- [2] D. Plummer, J.C. McConnel, P.B. Shepson, D.R. Hastie, H. Niki, *Atmos. Environ.* 30 (1996) 2195–2218.
- [3] J.A. Logan, *J. Geophys. Res.-Atmos.* 90 (ND6) (1985) 463–482.
- [4] J.H. Seinfeld, *Atmospheric Chemistry and Physics of Air Pollution*, Wiley, New York, 1986, p. 738.
- [5] W.P.L. Carter, Development of ozone reactivity scales for volatile organic compounds, EPA Rep. Atmos. Res. and Exposure Assessment Lab., Offic. of Res. and Dev., US Environmental Protection Agency, Research Triangle Park, NC, 1991, 84 pp.
- [6] W.P.L. Carter, *J. Air Waste Manage. Assoc.* 44 (1994) 881–899.
- [7] W.L. Chameides, F. Fehsenfeld, M.O. Rodgers, C. Cardelino, J. Martinez, D. Parrish, W. Lonneman, D.R. Lawson, R.A. Rasmussen, P. Zimmerman, J. Greenberg, P. Middleton, T. Wang, *J. Geophys. Res.* 97 (D5) (1992) 6037–6055.
- [8] C. Cardelino, W.L. Chameides, *J. Air Waste Manage. Soc.* 45 (1995) 161–180.
- [9] R. Atkinson, D.L. Baulch, R.A. Cox, R.F. Hampson Jr., J.A. Kerr Jr., J. Troe Jr., *J. Phys. Chem. Ref. Data* 21 (1992) 1125–1568 Suppl. 4.
- [10] W.B. DeMore, S.P. Sander, D.M. Golden, R.F. Hampson, M.J. Kurylo, C.J. Howard, A.R. Ravishankara, C.E. Kolb, M.J. Molina, NASA Panel for Data Evaluation: evaluation No. 12, JPL Publication 97-4, National Aeronautics and Space Administration, Pasadena, CA, 1997.
- [11] J.D. Fuentes, T.J. Gillespie, G. den Hartog, H.H. Newmann, *Agric. For. Met.* 62 (1992) 1–18.
- [12] P.J. Hanson, K. Rott, G.E. Taylor Jr., C.A. Gunderson Jr., S.E. Lindberg Jr., B.M. Ross-Todd Jr., *Atmos. Environ.* 23 (1989) 1783–1794.
- [13] A. Hofzumahaus, H.P. Dorn, J. Callics, U. Platt, D.H. Ehhalt, *Atmos. Environ. (A)* 25 (1991) 2017–2022.
- [14] G.H. Mount, F.L. Eisele, *Science* 256 (1992) 1187–1190.
- [15] R.J. O'Brian, T.M. Hard, *Adv. Chem. Series* 232 (1993) 323–371.
- [16] B.J. Finlayson-Pitts, J.N. Pitts Jr., *Atmospheric Chemistry: Fundamentals and Experimental Techniques*, Wiley, Toronto, 1986, pp. 110, 113, 143, 147, 151, 154–155.
- [17] N.J. Bunce, J.S. Nakai, M. Yawching, *Chemosphere* 22 (1991) 305–315.
- [18] J.E. Frederick, D. Lubin, *J. Geophys. Res.* 93 (D4) (1988) 3825–3832.
- [19] U. Platt, M. Rateike, W. Junkerman, J. Rudolph, D.H. Ehhalt, *J. Geophys. Res.-Atmos.* 93 (ND5) (1988) 5159–5166.
- [20] H.P. Dorn, J. Callics, U. Platt, D.H. Ehhalt, *Tellus* 40B (1988) 437–445.
- [21] D.M.L. Sills, W.J. Moroz, 89th Annual Meeting, Air and Waste Management Association, Nashville, TN, June 23–28, 1996, Extended Abstract # 96-TP23B.05.
- [22] G. Lammel, J.N. Cape, *Chem. Soc. Rev.* 25 (1996) 361–369.
- [23] S. Sillman, P.J. Samson, *J. Geophys. Res.* 100 (D6) (1995) 11497–11508.